

Shared Subspace Models for Multi-Group Covariance Estimation *

Alexander Franks and Peter Hoff

March 29, 2022

Abstract

We develop a model-based method for evaluating heterogeneity among several $p \times p$ covariance matrices in the large p , small n setting. This is done by assuming a spiked covariance model for each group and sharing information about the space spanned by the group-level eigenvectors. We use an empirical Bayes method to identify a low-dimensional subspace which explains variation across all groups and use an MCMC algorithm to estimate the posterior uncertainty of eigenvectors and eigenvalues on this subspace. The implementation and utility of our model is illustrated with analyses of high-dimensional multivariate gene expression and metabolomics data.

Keywords: covariance estimation; spiked covariance model; Stiefel manifold; Grassmann manifold; large p , small n ; high-dimensional data; empirical Bayes.

*Alexander M. Franks is a Moore/Sloan Data Science and WRF Innovation in Data Science Postdoctoral Fellow (amfranks@uw.edu). Peter D. Hoff is a Professor in the Department of Statistical Sciences at Duke University (peter.hoff@duke.edu). This work was partially supported by the Washington Research Foundation Fund for Innovation in Data-Intensive Discovery, the Moore/Sloan Data Science Environments Project at the University of Washington and NSF grant DMS-1505136. The authors are grateful to Dr. Daniel Promislow (Department of Pathology, University of Washington), Dr. Jessica Hoffman (University of Alabama at Birmingham) and Dr. Julie Josse (INRIA) for sharing data and ideas which contributed to framing of this paper.

1 Introduction

Multivariate data is often partitioned into groups, each of which represent samples from populations with distinct but possibly related distributions. Although historically the primary focus has been on identifying mean-level differences between populations, there has been a growing need to identify differences in population covariances as well. For instance, in case-control studies, mean-level effects may be small relative to subject variability; distributional differences between groups may still be evident as differences in the covariances between features. Even when mean-level differences are detectable, better estimates of the covariability of features across groups may lead to an improved understanding of the mechanisms underlying these apparent mean-level differences. Further, accurate covariance estimation is an essential part of many prediction tasks (e.g. quadratic discriminant analysis). Thus, evaluating heterogeneity between covariance matrices can be an important complement to more traditional analyses for estimating differences in means across groups.

To address this need, we develop a novel method for multi-group covariance estimation. Our method exploits the fact that in many natural systems, high dimensional data is often very structured and thus can be best understood on a lower dimensional subspace. For example, with gene expression data, the effective dimensionality is thought to scale with the number of gene regulatory modules, not the number of genes themselves [Heimberg et al., 2016]. As such, differences in gene expression across groups should be expressed in terms of differences between these regulatory modules rather than strict differences between expression levels. Such differences can be examined on a subspace that reflects the correlations resulting from these modules. In contrast to most existing approaches for group covariance estimation, our approach is to directly infer such subspaces from groups of related data.

Some of the earliest approaches for multi-group covariance estimation focus on estimation in terms of spectral decompositions. Flury [1987] developed estimation and testing procedures for the “common principal components” model, in which a set of covariance matrices were assumed to share the same eigenvectors. Schott [1991, 1999] considered cases in which only certain eigenvectors are shared across populations, and Boik [2002] described an even more general model in which eigenvectors can be shared between some or all of the groups. More recently, Hoff [2009a], noting that eigenvectors are unlikely to be shared exactly between groups, introduced a hierarchical model for eigenvector shrinkage based on the matrix Bingham distribution. There has also been a significant interest in estimating covariance matrices using Gaussian graphical models. For Gaussian graphical

models, zeros in the precision matrix correspond to conditional independencies between pairs of features given the remaining features [Meinshausen and Bühlmann, 2006]. Danaher et al. [2014] extended existing work in this area to the multi-group setting, by pooling information about the pattern of zeros across precision matrices.

Another popular method for modeling relationships between high-dimensional multivariate data is partial least squares regression (PLS) [Wold et al., 2001]. This approach, which is a special case of a bilinear factor model, involves projecting the data onto a lower dimensional space which maximizes the similarity of the two groups. This technique does not require the data from each group to share the same feature set. A common variant for prediction, partial least squares discriminant analysis (PLS-DA) is especially common in chemometrics and bioinformatics [Barker and Rayens, 2003]. Although closely related to the approaches we will consider here, the primarily goal of PLS-based models is to create regression or discrimination models, not to explicitly infer covariance matrices from multiple groups of data. Nevertheless, the basic idea that data can often be well represented on a low dimensional space is an appealing one that we leverage.

In this paper we propose a multi-group covariance estimation model by sharing information about the subspace spanned by group-level eigenvectors. The shared subspace assumption can be used to improve estimates and facilitate the interpretation of differences between covariance matrices across groups. For each group, we assume “the spiked covariance model” (also known as the “partial isotropy model”), a well studied variant of the factor model [Mardia et al., 1980, Johnstone, 2001]. In Section 2 we briefly review the behavior of spiked covariance models for estimating a single covariance matrix and then introduce our extension to the multi-group setting. In Section 3 we describe an empirical Bayes algorithm for inferring the shared subspace and estimating the posterior distribution of the covariance matrices of the data projected onto this subspace.

In Section 4 we investigate the behavior of this class of models in simulation and demonstrate how the shared subspace assumption is widely applicable, even when there is little similarity in the covariance matrices across groups. In particular, independent covariance estimation is equivalent to shared subspace estimation with a sufficiently large shared subspace. In Section 5 we use an asymptotic approximation to describe how shared subspace inference reduces bias when both p and n are large. Finally, In Section 6 we demonstrate the utility of a shared subspace model in an analysis of gene expression data from juvenile leukemia patients . Despite the large feature size ($p > 3000$) and small sample size ($n < 100$ per group), we identify interpretable similarities and differences in gene covariances on a low dimensional subspace. Finally, we conclude with a brief

exploration of heterogeneity in metabolomic data from a study on aging in the fly species *Drosophila melanogaster*.

2 A Shared Subspace Spiked Covariance Model

Suppose a random matrix S has a possibly degenerate $\text{Wishart}(\Sigma, n)$ distribution with density given by

$$p(S|\Sigma, n) \propto l(\Sigma : S) = |\Sigma|^{-n/2} \text{etr}(-\Sigma^{-1}S/2), \quad (1)$$

where $\Sigma \in \mathcal{S}_p^+$ and n may be less than p . Such a likelihood results from S being, for example, a residual sum of squares matrix from a multivariate regression analysis. In this case, n is the number of independent observations minus the rank of the design matrix. The spiked principal components model (spiked PCA) studied by Johnstone [2001] and others assumes that

$$\Sigma = \sigma^2(U\Lambda U^T + I) \quad (2)$$

where for $r \ll p$, Λ is an $r \times r$ diagonal matrix and $U \in \mathcal{V}_{p,r}$, where $\mathcal{V}_{p,r}$ is the Stiefel manifold consisting of all $p \times r$ orthonormal matrices in \mathbb{R}^p , so that $U^T U = I_r$. The spiked covariance formulation is appealing because it explicitly partitions the covariance matrix into a tractable low rank “signal” and isotropic “noise”.

Classical results for parametric models (e.g., Kiefer and Schwartz [1965]) imply that asymptotically in n for fixed p , an estimator will be consistent for a spiked population covariance as long as the assumed number of spikes (eigenvalues larger than σ^2) is greater than or equal to the true number. However, when p is large relative to n , as is the case for the examples considered here, things are more difficult. Under the spiked covariance model, it has been shown that if $p/n \rightarrow \alpha > 0$ as $n \rightarrow \infty$, the k th largest eigenvalue of $S/(n\sigma^2)$ will converge to an upwardly biased version of $\lambda_k + 1$ if λ_k is greater than $\sqrt{\alpha}$ [Baik and Silverstein, 2006, Paul, 2007]. This has led several authors to suggest estimating Σ via shrinkage of the eigenvalues of the sample covariance matrix. In particular, in the setting that σ^2 is known, Donoho et al. [2013] propose estimating all eigenvalues whose sample estimates are smaller than $\sigma^2(1 + \sqrt{\alpha})^2$ by σ^2 , and shrinking the larger eigenvalues in a way that depends on the particular loss function being used. These shrinkage functions are shown to be asymptotically optimal in the $p/n \rightarrow \alpha$ setting.

Note that covariance estimators of this form are are equivariant with respect to rotations and scale changes. The situation should be different, however, when we are interested in estimating

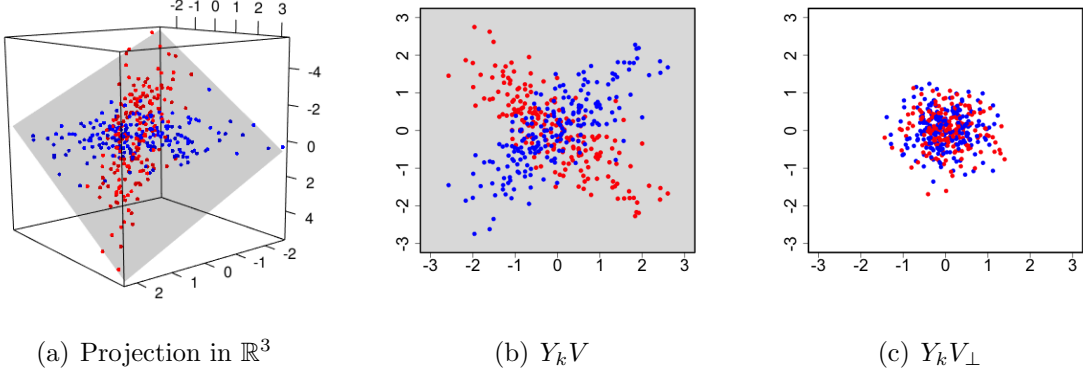


Figure 1: Two groups of four-dimensional data (red and blue) projected into different subspaces. a) To visualize Y_k we can project the data into \mathbb{R}^3 . In this illustration, the distributional differences between the groups are confined to a two-dimensional shared subspace (VV^T , grey plane). b) The data projected onto the two-dimensional shared subspace, Y_kV , have covariances Ψ_k that differ between groups. c) The orthogonal projection, Y_kV_{\perp} has isotropic covariance, $\sigma_k^2 I$, for all groups.

multiple covariance matrices from distinct but related groups. Here, group-level equivariance to rotations is an unreasonable assumption; both eigenvalue *and* eigenvector shrinkage can play an important role in improving covariance estimates. Consider multi-group covariance estimation based on K matrices, Y_1, \dots, Y_K , where Y_k is assumed to be an n_k by p matrix of mean-zero normal data, typically with $n_k \ll p$. Then, $Y_k^T Y_k = S_k$ has a (degenerate) Wishart distribution as in Equation 1. To improve estimation, we seek estimators of each covariance matrix, $\hat{\Sigma}_k$, that may depend on data from all groups. To this end, we extend the spiked covariance model to grouped data, by assuming that the anisotropic variability from each group occurs on a common low dimensional subspace. Specifically, we posit that the covariance matrix for each group can be written as

$$\Sigma_k = V \Psi_k V^T + \sigma_k^2 I, \quad (3)$$

where the columns of $V \in \mathcal{V}_{p,s}$, with $s \ll p$, determine a subspace shared by all groups. Throughout this paper we will denote to the shared subspace as $VV^T \in \mathcal{G}_{p,s}$, where $\mathcal{G}_{p,s}$ is the Grassmann manifold consisting of all s -dimensional linear subspaces of \mathbb{R}^p [Chikuse, 2012]. Although V is only identifiable up to right rotations, the matrix VV^T , which defines the plane of variation shared by all groups, is identifiable. Later, to emphasize the connection to the spiked PCA model (2), we will write Ψ_k in terms of its eigendecomposition, $\Psi_k = O_k \Lambda_k O_k^T$, where O_k are eigenvectors and Λ_k are the eigenvalues of Ψ_k (see Section 3.2).

Note that for a shared subspace model, $V^T \Sigma_k V = \Psi_k + \sigma_k^2 I$ is an anisotropic s -dimensional

covariance matrix for the projected data, $Y_k V$. In contrast, the data projected onto the orthogonal space, $Y_k V_{\perp}$, is isotropic for all groups. In Figure 1 we provide a simple illustration using simulated 4-dimensional data from two groups. In this example, the differences in distribution between the groups of data can be expressed on a two dimensional subspace spanned by the columns of $V \in \mathcal{V}_{4,2}$. Differences in the correlations between the two groups manifest themselves on this shared subspace, whereas only the magnitude of the isotropic variability can differ between groups on the orthogonal space. Thus, a shared subspace model can be viewed as a covariance partition model, where one partition includes the anisotropic variability from all groups and the other partition is constrained to the isotropic variability from each group. This isotropic variability is often characterized as measurement noise.

3 Empirical Bayes Inference

In this section we outline an empirical Bayes approach for estimating a low-dimensional shared subspace and the covariance matrices of the data projected onto this space. As we discuss in Section 4, if the spiked covariance model holds for each group individually, then the shared subspace assumption also holds, where the shared subspace is simply the span of the group-specific eigenvectors, U_1, \dots, U_K . In practice, we can usually identify a shared subspace of dimension $s \ll p$ that preserves most of the variation in the data. Our primary objective is to identify the “best” shared subspace of fixed dimension $s < p$. In Section 3.1 we describe an expectation-maximization algorithm for estimating the maximum marginal likelihood of the shared subspace, VV^T . This approach is computationally tractable for high-dimensional datasets. Given an inferred subspace, we then seek estimators for the covariance matrices of the data projected onto this space. Because seemingly large differences in the point estimates of covariance matrices across groups may not actually reflect statistically significant differences, in Section 3.2 we also describe a Gibbs sampler that can be used to generate estimates of the projected covariance matrices, Ψ_k , and their associated uncertainty. Later, in Section 4 we discuss strategies for inferring an appropriate value for s and explore how shared subspace models can be used for exploratory data analysis by visualizing covariance heterogeneity on two or three dimensional subspaces.

3.1 Estimating the Shared Subspace

In this section we describe a maximum marginal likelihood procedure for estimating the shared subspace, VV^T , based on the expectation-maximization (EM) algorithm. The full likelihood for the shared subspace model can be written as

$$\begin{aligned}
p(S_1, \dots, S_K | \Sigma_k, n_k) &\propto \prod_{k=1}^K |\Sigma_k|^{-n_k/2} \text{etr}(-\Sigma_k^{-1} S_k/2) \\
&\propto \prod_{k=1}^K |\Sigma_k|^{-n_k/2} \text{etr}(-(\sigma_k^2 (V\Psi_k V^T + I))^{-1} S_k/2) \\
&\propto \prod_{k=1}^K |\Sigma_k|^{-n_k/2} \text{etr}(-[V(\Psi_k + I)^{-1}/\sigma_k^2 V^T + (I - VV^T)/\sigma_k^2] S_k/2) \\
&\propto \prod_{k=1}^K (\sigma_k^2)^{-n_k(p-s)/2} |M_k|^{-n_k/2} \text{etr}(-[VM_k^{-1}V^T + \frac{1}{\sigma_k^2}(I - VV^T)] S_k/2), \quad (4)
\end{aligned}$$

where we define $M_k = \sigma_k^2(\Psi_k + I)$. The log-likelihood in V (up to an additive constant) is

$$\begin{aligned}
l(V) &= \sum_k \text{tr}(-VM_k^{-1}V^T + VV^T/\sigma_k^2) S_k/2 \\
&= \frac{1}{2} \sum_k \text{tr}\left((\frac{1}{\sigma_k^2}I - M_k^{-1})V^T S_k V\right). \quad (5)
\end{aligned}$$

We maximize the marginal likelihood of V with an EM algorithm, where M_k^{-1} and $\frac{1}{\sigma_k^2}$ are considered the “missing” parameters. We assume independent Jeffreys’ prior distributions for both σ_k^2 and M_k . Jeffreys’ prior for these quantities corresponds to $p(\sigma_k^2) \propto 1/\sigma_k^2$ and $p(M_k) \propto |M_k|^{-(s+1)/2}$. From the likelihood it can easily be shown that the conditional posterior for M_k is

$$p(M_k|V) \propto |M_k|^{(n_k+s+1)/2} \text{etr}(-(M_k^{-1}V^T S_k V)/2)$$

which is an inverse-Wishart($V^T S_k V, n_k$) distribution. The conditional posterior distribution of σ_k^2 is simply

$$p(\sigma^2|V) \propto (\sigma_k^2)^{-n_k(p-s)/2-1} \text{etr}(-(I - VV^T)S_k/[2\sigma_k^2])$$

which is an inverse-gamma($n_k(p-s)/2, \text{tr}[(I - VV^T)S_k]/2$) distribution. Based on these results, we complete the following steps for each iteration t of the EM algorithm until convergence:

1. For each k , compute relevant conditional expectations:

$$(a) E[M_k^{-1}|V_{(t-1)}] = n_k(V_{(t-1)}^T S_k V_{(t-1)})^{-1}$$

$$(b) E[\frac{1}{\sigma_k^2} | V_{(t-1)}] = \frac{n_k(p-s)}{\text{tr}[(I - V_{(t-1)} V_{(t-1)}^T) S_k]}$$

$$2. \text{ Compute } V_t = \arg \max_V \sum_k \text{tr} \left(-VE[M^{-1}|V_{(t-1)}]V^T + E[\frac{1}{2\sigma_k^2}|V_{(t-1)}]VV^T \right) S_k / 2)$$

For the second step (“M-step”), we use a numerical optimization algorithm based on the Cayley transform to preserve the orthogonality constraints in V [Wen and Yin, 2013]. Importantly, the complexity of this algorithm is dominated by the dimension of the shared subspace, not the number of features. Thus, our approach is computationally efficient for relatively small values of s , even when p is large.

Evaluating Goodness of Fit: If V is a basis for a shared subspace, then for each group, most of the non-isotropic variation in Y_k should be preserved when projecting the data onto this space. To characterize the extent to which this is true for different groups, we propose a simple estimator for the proportion of “signal” variance that lies on a given subspace. Specifically, we use the following statistic for the ratio of the sum of the first s eigenvalues of $V^T \Sigma_k V$ to the sum of the first s eigenvalues of Σ_k :

$$\gamma(Y_k : V, \sigma_k^2) = \frac{\|Y_k V\|_F / n_k}{\max_{\tilde{V} \in \mathcal{V}_{p,s}} \|Y_k \tilde{V}\|_F / n_k - \sigma_k^2 ps / n_k} \quad (6)$$

where $\|\cdot\|_F$ is the Frobenius norm. Our motivation for this statistic is the fact that if $\Sigma_k = V \Psi_k V^T + \sigma_k^2 I$ then $\gamma(Y_k : V, \sigma_k^2) \approx 1$. We establish this in an asymptotic regime where s is fixed, $p, n_k \rightarrow \infty$ and $p/n_k = \alpha_k$ constant.

First, since s is fixed and n_k is growing, the numerator, $\|Y_k V\|_F / n_k$, is a consistent estimator for the sum of the eigenvalues of $V^T \Sigma_k V$. The denominator, $\max_{\tilde{V} \in \mathcal{V}_{p,s}} \|Y_k \tilde{V}\|_F / n_k$ is equivalent to the sum of the first s eigenvalues of the sample covariance matrix S_k / n_k . With $\hat{\lambda}_i^{(k)}$ the i -th eigenvalue of S_k / n_k , Baik and Silverstein [2006] demonstrated that asymptotically as $p, n_k \rightarrow \infty$ with $p/n_k = \alpha_k$ fixed

$$\begin{aligned} \hat{\lambda}_i^{(k)} &\rightarrow \lambda_i^{(k)} \left(1 + \frac{\sigma_k^2 \alpha_k}{\lambda_i^{(k)} - 1} \right) \\ &\approx \lambda_i^{(k)} + \sigma_k^2 \frac{p}{n_k} \end{aligned} \quad (7)$$

where the approximation in the second line is due to the fact that $\lambda_k / (\lambda_k - 1) \approx 1$ for λ_k large. Thus, $\sum_i \hat{\lambda}_i^{(k)} \approx \sum_i \lambda_i^{(k)} + \sigma_k^2 ps / n_k$ and $\max_{\tilde{V} \in \mathcal{V}_{p,s}} \|Y_k \tilde{V}\|_F / n_k - \sigma_k^2 ps / n_k$ is a reasonable approximation to the sum of the first s eigenvalues of Σ_k . Alternatively, when λ_k is small, a better approximation may be obtained by solving the quadratic equation implied by the first line of Equation 7.

As a consequence, the proposed statistic will be close to one for all groups when VV^T is a shared subspace for the data and smaller if not. The metric provides a useful indicator of which groups can be reasonably compared on a given subspace and which groups cannot. In practice, we estimate a shared subspace \hat{V} and the isotropic variances $\hat{\sigma}_k^2$ using EM and compute the plug-in estimate $\gamma(Y_k : \hat{V}, \hat{\sigma}_k^2)$. When this statistic is small for some groups, it may suggest that the rank s of the inferred subspace needs to be larger to capture the variation in all groups. We investigate this in Section 4, by computing the goodness of fit statistic for inferred subspaces of different dimensions on a single dataset. In Section 6, we compute the estimates for subspaces inferred with real biological data.

3.2 Inference for Projected Covariance Matrices

The EM algorithm presented in the previous section yields point estimates for VV^T , Ψ_k , and σ_k^2 but does not lead to natural uncertainty quantification for these estimates. In this section, we assume that the subspace VV^T is fixed and known and demonstrate how we can estimate the posterior distribution for Ψ_k . Note that when the subspace is known, the posterior distribution of Σ_k is conditionally independent from the other groups, so that we can independently estimate the conditional posterior distributions for each group.

There are many different ways in which we could choose to parameterize Ψ_k . Building on recent interest in the spiked covariance model [Donoho et al., 2013, Paul, 2007] we propose a tractable MCMC algorithm by specifying priors on the eigenvalues and eigenvectors of Ψ_k . By modeling the eigenstructure, we can now view each covariance Σ_k in terms of the original spiked principal components model. Equation 3, written as a function of V , becomes

$$\begin{aligned}\Psi_k &= O_k \Lambda_k O_k^T \\ \Sigma_k &= V \Psi_k V^T + \sigma_k^2 I.\end{aligned}\tag{8}$$

Here, we allow Ψ_k to be of rank $r \leq s$ dimensional covariance matrix on the s -dimensional subspace. Thus, Λ_k is an $r \times r$ diagonal matrix of eigenvalues, and $O_k \in \mathcal{V}_{s,r}$ is the matrix of eigenvectors of Ψ_k . For any individual group, this corresponds to the original spiked PCA model (Equation 2) with $U_k = VO_k \in \mathcal{V}_{p,r}$. Differentiating the ranks r and s is helpful because it enables us to independently specify a subspace common to all groups and the possibly lower rank features on this space that are specific to individual groups. Although our model is most useful when the covariance matrices

are related across groups, we can also use this formulation to specify models for multiple unrelated spiked covariance models. We explore this in detail in Section 4. In Section 6 we introduce a shared subspace model with additional structure on the eigenvectors and eigenvalues of Ψ_k to facilitate interpretation of covariance heterogeneity on a two-dimensional subspace.

The likelihood for Σ_k given the sufficient statistic $S_k = Y_k Y_k^T$ is given in Equation 1. For the spiked PCA formulation, we must rewrite this likelihood in terms of V , O_k , Λ_k and σ_k^2 . First note that by the Woodbury matrix identity

$$\begin{aligned}\Sigma_k^{-1} &= (\sigma_k^2(U_k \Lambda_k U_k^T + I))^{-1} \\ &= \frac{1}{\sigma_k^2}(U_k \Lambda_k U_k^T + I)^{-1} \\ &= \frac{1}{\sigma_k^2}(I - U_k \Omega_k U_k^T),\end{aligned}\tag{9}$$

where the diagonal matrix $\Omega = \Lambda(I + \Lambda)^{-1}$, e.g. $\omega_i = \frac{\lambda_i}{\lambda_i + 1}$. Further,

$$\begin{aligned}|\Sigma_k| &= (\sigma_k^2)^p |U_k \Lambda_k U_k^T + I| \\ &= (\sigma_k^2)^p |\Lambda_k + I| \\ &= (\sigma_k^2)^p \prod_{i=1}^r (\lambda_i + 1) \\ &= (\sigma_k^2)^p \prod_{i=1}^r (1 - \omega_i),\end{aligned}\tag{10}$$

where the second line is due to Sylvester's determinant theorem. Now, the likelihood of V , O_k , Λ_k and σ_k^2 is available from Equation 1 by substituting the appropriate quantities for Σ_k^{-1} and $|\Sigma_k|$ and replacing U_k with VO_k :

$$L(\sigma_k^2, V, O_k \Omega_k : Y_k) \propto (\sigma_k^2)^{-n_k p/2} \text{etr}\left(-\frac{1}{2\sigma_k^2} S_k\right) \left(\prod_{i=1}^r (1 - \omega_{ki})\right)^{n_k/2} \text{etr}\left(\frac{1}{2\sigma_k^2} (VO_k \Omega_k O_k^T V^T) S_k\right).\tag{11}$$

We use conjugate and semi-conjugate priors for the parameters O_k , σ_k^2 and Ω_k to facilitate inference via a Gibbs sampling algorithm. In the absence of specific prior information, invariance considerations suggest the use of priors that lead to equivariant estimators. Below we describe our choices for the prior distributions of each parameter and the resultant conditional posterior distributions.

Conditional distribution of σ_k^2 : From Equation 11 it is clear that the the inverse-gamma class of prior distributions is conjugate for σ_k^2 . We chose a default prior distribution for σ_k^2 that is equivariant with respect to scale changes. Specifically, we use Jeffreys' prior, an improper prior with

density $p(\sigma_k^2) \propto 1/\sigma_k^2$. Under this prior, straightforward calculations show that the full conditional distribution of σ_k^2 is inverse-gamma($n_k p/2, \text{tr}[S_k(I - U_k \Omega_k U_k)/2]$), where $U_k = VO_k$.

Conditional distribution of O_k : Given the likelihood from Equation 11, it is easy to show that the class of Bingham distributions are conjugate for O_k [Hoff, 2009a,b]. Again, invariance considerations lead us to use a rotationally invariant uniform probability measure on $\mathcal{V}_{s,p}$. Under this uniform prior, the full conditional distribution of O_k has a density proportional to the likelihood

$$p(O_k | \sigma_k^2, U_k, \Omega_k) \propto \text{etr}(\Omega_k O_k^T V^T [S_k / (2\sigma_k^2)] V O_k). \quad (12)$$

This is a $\text{Bingham}(\Omega, V^T S_k V / (2\sigma^2))$ distribution on $\mathcal{V}_{s,r}$ [Khatri and Mardia, 1977]. A Gibbs sampler to simulate from this distribution is given in Hoff [2009b].

Together, the prior for σ_k^2 and O_k leads to conditional (on V) Bayes estimators $\hat{\Sigma}(V^T S_k V)$ that are equivariant with respect to scale changes and rotations on the subspace spanned by V , so that $\hat{\Sigma}(aWV^T S_k V W^T) = aW\hat{\Sigma}(V^T S_k V)W$ for all $a > 0$ and $W \in \mathcal{O}_s$ (assuming an invariant loss function). Interestingly, if Ω_k were known (which it is not), then for a given invariant loss function the Bayes estimator under this prior minimizes the (frequentist) risk among all equivariant estimators [Eaton, 1989].

Conditional distribution for Ω_k : Here we specify the conditional distribution of the diagonal matrix $\Omega_k = \Lambda_k(I + \Lambda_k)^{-1} = \text{diag}(\omega_{k1}, \dots, \omega_{kr})$. We consider a uniform(0,1) prior distribution for each element of Ω , or equivalently, an $F_{2,2}$ prior distribution for the elements of Λ . The full conditional distribution of an element ω_i of Ω is proportional to the likelihood function

$$p(\omega_{ki} | V, O_k, S_k) \propto_{\omega_{ki}} \left(\prod_{i=1}^r (1 - \omega_{ki})^{n_k/2} \right) \text{etr}\left(\frac{1}{2\sigma_k^2} (V O_k \Omega_k O_k^T V^T) S_k\right) \quad (13)$$

$$\propto (1 - \omega_{ki})^{n/2} e^{c_{ki} \omega_{ki} n/2}, \quad (14)$$

where $c_{ki} = u_{ki}^T S_k u_{ki} / (n_k \sigma_k^2)$ and u_{ki} is column i of $U_k = VO_k$. While not proportional to a density belonging to a standard class of distributions, we can sample from the corresponding univariate distribution numerically. The behavior of this distribution is straightforward to understand: if $c_{ki} \leq 1$, then the function has a maximum at $\omega_{ki} = 0$, and decays monotonically to zero as $\omega_{ki} \rightarrow 1$. If $c_{ki} > 1$ then the function is uniquely maximized at $(c_{ki} - 1)/c_{ki} \in (0, 1)$. To see why this makes sense, note that the likelihood is maximized when the columns of U_k are equal to the eigenvectors of S_k corresponding to its top r eigenvalues [Tipping and Bishop, 1999]. At this value

of U_k , c_{ki} will then equal one of the top r eigenvalues of $S_k/(n_k\sigma_k^2)$. In the case that $n_k \gg p$, we expect $S_k/(n_k\sigma_k^2) \approx \Sigma_k/\sigma_k^2$, the true (scaled) population covariance, and so we expect c_{ki} to be near one of the top r eigenvalues of Σ_k/σ_k^2 , say $\lambda_{ki} + 1$. If indeed Σ_k has r spikes, then $\lambda_{ki} > 0$, $c_{ki} \approx \lambda_{ki} + 1 > 1$, and so the conditional mode of w_{ki} is approximately $(c_{ki} - 1)/c_{ki} = \lambda_{ki}/(\lambda_{ki} + 1)$, the correct value. On the other hand, if we have assumed the existence of a spike when there is none, then $\lambda_{ki} = 0$, $c_{ki} \approx 1$ and the Bayes estimate of w_{ki} will be shrunk towards zero, as it should be.

4 Simulation Study

We start with an example demonstrating how a shared subspace model can be used to identify statistically significant differences between covariance matrices on a low dimensional subspace. Here, we simulate $K = 5$ groups of data from the shared subspace spiked covariance model with $p = 200$, $s = r = 2$, $\sigma_k^2 = 1$, and $n_k = 50$. We fix the first eigenvalue of Ψ_k from each group to $\lambda_1 = 100$ and vary λ_2 . For this two dimensional shared subspace model we summarize Ψ_k in terms of its eigendecomposition by computing posterior distributions for the log eigenvalue ratio, $\log(\frac{\lambda_1}{\lambda_2})$, with $\lambda_1 > \lambda_2$, and the angle of the first eigenvector on this subspace, $\arctan(\frac{O_{12}}{O_{21}})$, relative to the first column of V .

Figure 4 depicts the 95% posterior regions for these quantities from a single simulation. Dots correspond to the true log ratios and orientations of $\hat{V}^T \Sigma_k \hat{V}$, where \hat{V} is the maximum marginal likelihood for V . To compute the posterior regions, we iteratively remove posterior samples corresponding to the vertices of the convex hull until only 95% of the original samples remain. Non-overlapping posterior regions provide evidence that differences in the covariances are “statistically significant” between groups. In this example, the ratio of the eigenvalues of the true covariance matrices were 10 (black and red groups), 3 (green and blue groups) and 1 (cyan group). Larger eigenvalue ratios correspond to more correlated contours and a value of 1 implies isotropic covariance. Note that for the smaller eigenvalue ratio of 3, there is larger uncertainty about the orientation of the primary axis. When the ratio is one, as is the case for the cyan colored group, there is no information about the orientation of the primary axis since the contours are spherical.

To demonstrate the overall validity of the shared subspace approach, we compute the frequentist coverage of these 95% bayesian credible regions for the eigenvalue ratio and primary axis orientation using one thousand simulations. For the two groups with eigenvalue ratio $\lambda_1/\lambda_2 = 3$ the frequentist

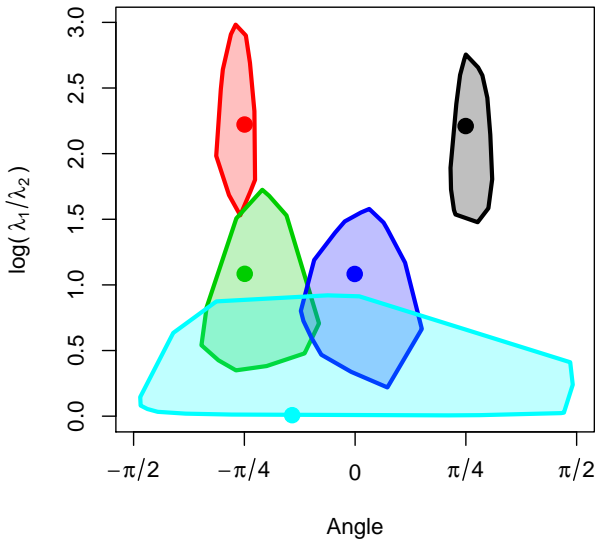


Figure 2: a) 95% posterior regions for the log of the ratio of eigenvalues, $\log(\frac{\lambda_1}{\lambda_2})$, of Ψ_k and the orientation of the principal axis on the space spanned by \hat{V} cover the truth in this simulation. Dots correspond to true data generating parameter values on $\hat{V}^T \Sigma_k \hat{V}$. Since V is only identifiable up to rotation, for this figure we find the Procrustes rotation that maximizes the similarity of \hat{V} to the true data generating basis. True eigenvalue ratios were 10 (red and black), 3 (green and blue) and 1 (light blue). True orientations were $\pi/4$ (black), $-\pi/4$ (red and green) and 0 (blue and cyan).

coverage was close to nominal at approximately 0.94. For the groups with $\lambda_1/\lambda_2 = 10$ the coverage was approximately 0.92. We did not evaluate the coverage for the group with $\lambda_1/\lambda_2 = 1$ (cyan) since this value is on the edge of the parameter space and is not covered by the 95% posterior regions as constructed. The slight under coverage for the other groups is likely due to the fact that we infer VV^T using maximum marginal likelihood, and thus ignore the extra variability due to the uncertainty about the shared subspace estimate.

4.1 Rank Selection and Model Misspecification

Naturally, shared subspace inference works well when the model is correctly specified. What happens when the model is not well specified? We explore this question in silico by simulating data from different data generating models and evaluating the efficiency of various covariance estimators. In all of the following simulations we evaluate covariance estimates using Stein's loss, $L_S(\Sigma_k, \hat{\Sigma}_k) =$

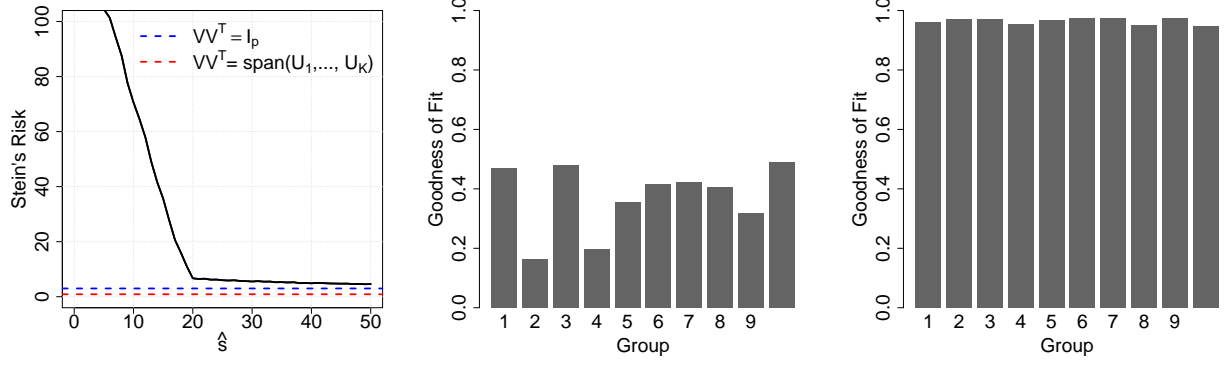
(a) Stein's risk vs \hat{s} (b) $\hat{s} = 5$ (c) $\hat{s} = 20$

Figure 3: a) Stein's risk as a function of the shared subspace dimension. Data from ten groups, with U_k generated uniformly on the Stiefel manifold $\mathcal{V}_{200,2}$. As $\hat{s} \rightarrow p$, the risk converges to the risk from independently estimated spiked covariance matrices (dashed blue line). The data also fit a shared subspace model with $s = rK$. If $VV^T = \text{span}(U_1, \dots, U_k)$ were known exactly, shared subspace estimation yields lower risk than independent covariance estimation (dashed red line). b) For a single simulated dataset, the goodness of fit statistic, $\gamma(Y_k : \hat{V}, \hat{\sigma}_k^2)$, when the assumed shared subspace is dimension $\hat{s} = 5$. c) For the same dataset, goodness of fit when the assumed shared subspace is dimension $\hat{s} = 20$. We can capture nearly all of the variability in each of the 10 groups using an $\hat{s} = rK = 20$ dimensional shared subspace.

$\text{tr}(\Sigma_k^{-1} \hat{\Sigma}_k) - \log |\Sigma_k^{-1} \Sigma_k| - p$. Since we compute multi-group estimates, we report the average Stein's loss $L(\Sigma_1, \dots, \Sigma_K; \hat{\Sigma}_1, \dots, \hat{\Sigma}_K) = \frac{1}{K} \sum_k L_S(\Sigma_k, \hat{\Sigma}_k)$. Under Stein's loss, the Bayes estimator is the inverse of the posterior mean of the precision matrix, $\hat{\Sigma}_k = E[\Sigma_k^{-1} | S_k]^{-1}$ which we estimate using MCMC samples.

We start by investigating the behavior of our model when we underestimate the true dimension of the shared subspace. In this simulation, we generate $K = 10$ groups of mean-zero normally distributed data with $p = 200$, $r = 2$, $s = p$ and $\sigma_k^2 = 1$. We fix the eigenvalues of Ψ_k to $(\lambda_1, \lambda_2) = (250, 25)$. Although the signal variance from each group individually is preserved on a two dimensional subspace, these subspaces are not similar across groups since the eigenvectors from each group are generated uniformly from the Stiefel manifold, $U_k \in \mathcal{V}_{p,r}$.

We use these data to evaluate how well the shared subspace estimator performs when we fit the data using a shared subspace model of dimension $\hat{s} < s$. In Figure 3(a) we plot Stein's risk as a function of \hat{s} , estimating the risk empirically using ten independent simulations per value of \hat{s} .

The dashed blue line corresponds to Stein’s risk for covariance matrices estimated independently. Independent covariance estimation is equivalent to shared subspace inference with $\hat{s} = p$ because this implies $VV^T = I_p$. Although the risk is large for small values of \hat{s} , as the shared subspace dimension increases to the dimension of the feature space, that is $\hat{s} \rightarrow p$, the risk for the shared subspace estimator quickly decreases. Importantly, it is always true that $\text{rank}([U_1, \dots, U_K]) \leq rK$ so it can equivalently be assumed that the data were generated from a shared subspace model with dimension $s = rK < p$. As such, even when there is little similarity between the eigenvectors from each group, the shared subspace estimator with $\hat{s} = rK$ will perform well, provided that we can identify a subspace, $\hat{V}\hat{V}^T$ that is close to $\text{span}([U_1, \dots, U_K])$. When $\hat{V}\hat{V}^T = \text{span}([U_1, \dots, U_K])$ exactly, shared subspace estimation outperforms independent covariance estimation (3(a), dashed red line).

From this simulation, it is clear that correctly specifying the dimension of the shared subspace is important for efficient covariance estimation. When the dimension of the shared subspace is too small, we accrue higher risk. The goodness of fit statistic, $\gamma(Y_k : \hat{V}, \hat{\sigma}_k^2)$, can be used to identify when a larger shared subspace is warranted. When \hat{s} is too small, $\gamma(Y_k : \hat{V}, \hat{\sigma}_k^2)$ will be substantially smaller than one for at least some of the groups, regardless of \hat{V} (e.g. Figure 3(b)). When \hat{s} is large enough, we are able to use maximum marginal likelihood to identify a shared subspace which preserves most of the variation in the data for all groups (Figure 3(c)). Thus, for any estimated subspace, the goodness of fit statistic can be used to identify the groups that can be fairly compared on this subspace and whether we would benefit from fitting a model with a larger value of \hat{s} .

Model Comparison and Rank Estimation: Clearly, correct specification for the rank of the shared subspace is important for efficient inference. So far in this section, we have assumed that the group rank, r , and shared subspace dimension, s , are fixed and known. In practice this is not the case. Prior to fitting a model we should estimate these quantities. Gavish and Donoho [2014] provide an asymptotically optimal (in mean squared error) singular value threshold for low rank matrix recovery with noisy data. We use their rank estimator, which is a function of the median singular value of the data matrix and the ratio $\alpha_k = \frac{p}{n_k}$, to estimate r . Although their estimator was derived for individual covariance estimation, we found that Gavish and Donoho’s estimator can also be applied to the pooled data to estimate s . Specifically, we concatenate the data from all groups to create an $(\sum_k n_k) \times p$ dimensional matrix and apply their rank estimator to this matrix to choose s .

Table 1: Stein’s risk (and 95% loss intervals) for different inferential models and data generating models with varying degrees of between-group covariance similarity. For each of $K = 10$ groups, we simulate data from three different types of shared subspace models. For each of these models, $p = 200$, $r = 2$, $\sigma_k^2 = 1$ and $n_k = 50$. We also fit the data using three different shared subspace models: a model in which s , r and VV^T are all estimated from the data (“adaptive”), a spiked covariance model in which the covariance matrices from each group are assumed to be identical ($\hat{\Sigma}_k = \hat{\Sigma}$) and a model in which we assume the data do *not* share a lower dimensional subspace across groups (i.e. $\hat{s} = p$). The estimators which most closely match the data generating model have the lowest risk (diagonal) but the adaptive estimator performs well relative to the alternative misspecified model.

		Inferential Model		
		Adaptive	$\hat{\Sigma}_k = \hat{\Sigma}$	$\hat{s} = p$
Data Model	$s = r = 2$	0.8 (0.7, 0.9)	2.1 (1.7, 2.6)	3.0 (2.9, 3.2)
	$s = r = 2, \Sigma_k = \Sigma$	0.8 (0.7, 0.9)	0.7 (0.6, 0.8)	3.0 (2.9, 3.2)
	$s = p = 200$	7.1 (6.2, 8.0)	138.2 (119, 153)	3.0 (2.9, 3.2)

Using these rank estimators, we conduct a simulation which demonstrates the relative performance of shared subspace group covariance estimation under different data generating models. In these simulations we assume the data have $p = 200$ features, $r = 2$ spikes, $\sigma_k^2 = 1$, and $n_k = 50$. We fix the non-zero eigenvalues of Ψ_k to $(\lambda_1, \lambda_2) = (250, 25)$. We consider three different shared subspace data models: 1) a low dimensional shared subspace model with $s = r = 2$; 2) a model in which the spiked covariance matrices from all groups are identical, e.g. $\Sigma_k = \Sigma = U\Lambda U^T + \sigma^2 I$; and 3) a full rank shared subspace model with $s = p = 200$. We simulate 100 independent datasets for each of these data generating mechanisms.

We estimated group-level covariance matrices from these datasets using three different variants of the shared subspace model. For each of these fits we estimate r . First, we estimate a single spiked covariance matrix from the pooled data and let $\hat{\Sigma}_k = \hat{\Sigma}$. Second, we fit the full rank shared subspace model. This corresponds to a procedure in which we estimate each spiked covariance matrix independently, since $s = p$ implies $VV^T = I_p$. Finally, we use an “adaptive” shared subspace estimator, in which we estimate both s , r and VV^T . In Table 1 we report the average Stein’s risk and corresponding 95% loss intervals for the estimates derived from each of these inferential models.

As expected, the estimates with the lowest risk are derived from the inferential model that

most closely match the data generating specifications. However, the adaptive estimator has small risk under model misspecification relative to the alternatives. For example, when $\Sigma_k = \Sigma$, the adaptive shared subspace estimator has almost four times smaller risk than the full rank estimator, in which each covariance matrix is estimated independently. When the data come from a model in which $s = p$, that is, the eigenvectors of Ψ_k are generated uniformly from $\mathcal{V}_{p,r}$, the adaptive estimator is over an order of magnitude better than the estimator which assumes no differences between groups. These results suggest that empirical Bayes inference for VV^T combined with the rank estimation procedure suggested by Gavish and Donoho [2014] can be widely applied to group covariance estimation because the estimator adapts to the amount of similarity across groups. Thus, shared subspace estimation can be an especially appropriate choice when the similarity between groups is not known a priori.

5 Reduction of Asymptotic Bias Via Pooling

Recently, there has been an interest in the asymptotic behavior of PCA-based covariance estimators in the setting in which $p, n \rightarrow \infty$ with $p/n = \gamma$ fixed. Specifically, in the spiked covariance model it is known that when p and n are both large, the leading eigenvalues of the sample covariance matrix are positively biased and the empirical eigenvectors form a non-zero angle with the true eigenvectors [Baik and Silverstein, 2006, Paul, 2007]. Although this fact also implies that the shared subspace estimators are biased, a major advantage of shared subspace inference over independent estimation of multiple covariance matrices is that we reduce the asymptotic bias by pooling information across groups. The bias reduction is especially large when there is significant heterogeneity in the first s eigenvectors of the projected covariance matrices.

Throughout section we assume K groups of data each with $n_k = n$ observations per group and s a fixed constant. First, note that if $\hat{V}\hat{V}^T$ corresponds to the true shared subspace, then estimates $\hat{\psi}_k$ derived using the methods presented in Section 3.2 will consistently estimate ψ_k as $n \rightarrow \infty$ regardless of whether p increases as well because $Y_k V$ has a fixed number of columns. For this reason, we focus explicitly on the accuracy of $\hat{V}\hat{V}^T$ (derived using the maximum marginal likelihood algorithm presented in Section 3.1) as a function of the number of groups K when both p and n are of the same order of magnitude and much larger than s . As an accuracy metric, we study the behavior of $\text{tr}(\hat{V}\hat{V}^T VV^T)/s$. This metric is bounded by zero and one and achieves a maximum of one if and only if $\hat{V}\hat{V}^T$ corresponds to the true shared subspace.

To start, we consider the simple case in which the data matrices Y_k are identically distributed with covariance $\Sigma_k = \Sigma$ of the shared-subspace form given in Equation 3 and $\sigma_k^2 = 1$. Without loss of generality we can let $\psi_k = \psi$ be a diagonal matrix (e.g. assume the columns of V align with the eigenvectors of Σ). In this case, for a single group the complete data likelihood of V (Equation 5) can be rewritten as

$$\begin{aligned}\ell(V) &= \frac{1}{2} \text{tr} \left(\left(\frac{1}{\sigma^2} I - M^{-1} \right) V^T S_k V \right) \\ &= \frac{1}{2} \text{tr} \left(D V^T S_k V \right).\end{aligned}$$

Since ψ is diagonal and $\sigma^2 = 1$, $M = \sigma^2(\psi + I)$ is diagonal and thus $D = (\frac{1}{\sigma^2} I - M^{-1})$ is also diagonal with entries $0 < d_i < 1$ of decreasing magnitude. Then, the solution to

$$\hat{V}^{(k)} = \underset{\tilde{V} \in \mathcal{V}_{p,s}}{\text{argmax}} \text{tr} \left(D \tilde{V}^T S_k \tilde{V} \right).$$

has $\hat{V}^{(k)}$ equal to the first s eigenvectors of S_k . This is maximized when the columns of V match the first empirical eigenvectors of S_k and has a maximum of $\sum_{i=1}^r d_i \ell_i$ where ℓ_i is the i th eigenvalue of S_k . As shown in Paul [2007], as long as $\lambda_i > 1 + \sqrt{\gamma}$ where λ_i is the i th eigenvalue of Σ_k , the asymptotic inner product between the i th sample eigenvector and the i th population eigenvector approaches a limit that is almost surely less than one

$$|\langle \hat{V}_i^{(k)}, V_i \rangle| \rightarrow \sqrt{\left(1 - \frac{\gamma}{(\lambda_i - 1)^2} \right) / \left(1 + \frac{\gamma}{(\lambda_i - 1)} \right)}$$

As such, for each independent estimate $\hat{V}^{(k)} \hat{V}^{(k)T}$, we can approximate the shared subspace accuracy as

$$\begin{aligned}\text{tr}(\hat{V}^{(k)} \hat{V}^{(k)T} V V^T) / s &= \frac{1}{s} \sum_{i=1}^s |\langle \hat{V}_i^{(k)}, V_i \rangle|^2 \\ &\approx \frac{1}{s} \sum_{i=1}^s \left(1 - \frac{\gamma}{(\lambda_i - 1)^2} \right) / \left(1 + \frac{\gamma}{(\lambda_i - 1)} \right).\end{aligned}\tag{15}$$

Naturally, when the groups are identically distributed, $V V^T$ should be estimated using the pooled data. In this simple case, it is easy to analytically express the improvement in subspace accuracy from pooling data across groups. The maximum likelihood estimate for $V V^T$ for the pooled data can be expressed as

$$\hat{V} = \underset{\tilde{V} \in \mathcal{V}_{p,s}}{\text{argmax}} \text{tr} \left(D \tilde{V}^T \left(\sum_{k=1}^K S_k \right) \tilde{V} \right)$$

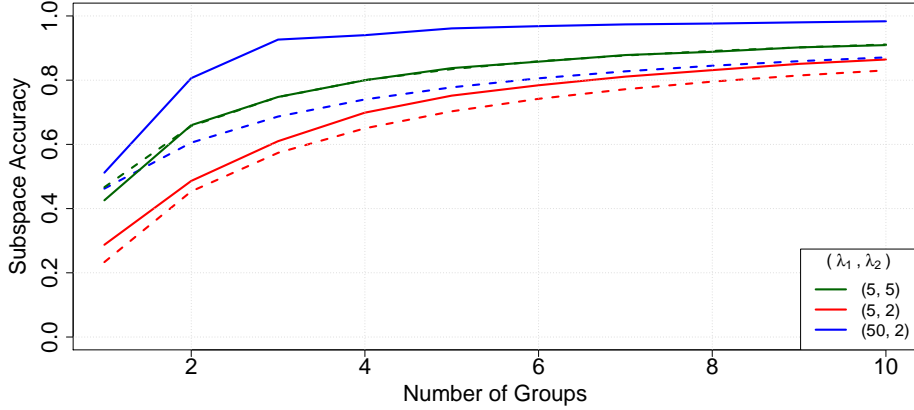


Figure 4: Subspace accuracy $\text{tr}(\hat{V}\hat{V}^T VV^T)/s$ (solid) and the asymptotics-based benchmark (dashed) as a function of K . When $\lambda_1 = \lambda_2$ (green), the assumptions used to derive the benchmark (identically distributed groups) are met and thus the subspace accuracy matches the benchmark. However, when the ratio λ_1/λ_2 is large, the subspace accuracy metric can far exceed this benchmark if there is significant variation in the eigenvectors of ψ_k across groups. Small increases in accuracy over the benchmark are seen for moderately anisotropic data (red) and large increases for highly anisotropic data (blue).

where $\sum_{k=1}^K S_k \sim \text{Wish}(\Sigma, Kn)$. Thus, in this example we can express the accuracy of $\hat{V}\hat{V}^T$ for the pooled estimator as:

$$\begin{aligned} \text{tr}(\hat{V}\hat{V}^T VV^T)/s &= \sum_{i=1}^s |\langle \hat{V}_i, V_i \rangle|^2 \\ &\approx \frac{1}{s} \sum_{i=1}^s \left(1 - \frac{\gamma}{K(\lambda_i - 1)^2} \right) / \left(1 + \frac{\gamma}{K(\lambda_i - 1)} \right). \end{aligned} \quad (16)$$

Here, the accuracy of the estimate depends on γ , K and the magnitude of the eigenvalues, with the bias decreasing as the number of groups K increases. Empirically, in the fully general setting in which ψ_k varies across groups we get bias reductions that scale similarly in K . This is supported by the results in Table 1 which show that when estimating groups of spiked covariance matrices using the shared subspace estimator there is a significant reduction in Stein's risk. Moreover, Equation 16 provides a useful benchmark for understanding the bias of shared subspace estimates.

In Figure 4 we depict the subspace accuracy metric $\text{tr}(\hat{V}\hat{V}^T VV^T)/s$ and benchmark $\frac{1}{s} \sum_{i=1}^s \left(1 - \frac{\gamma}{K(\lambda_i - 1)^2} \right) / \left(1 + \frac{\gamma}{K(\lambda_i - 1)} \right)$ for simulated multi-group data generated under the shared subspace model with $s = 2$, $n = 50$, $p = 200$ and three different sets of eigenvalues. For each covariance matrix, the eigenvectors of

ψ_k were sampled uniformly from Stiefel manifold $\mathcal{V}_{2,2}$. When ψ_k is isotropic (green) the subspace similarity metric closely matches the benchmark since the assumptions used to derive this asymptotic result are met. However, when the eigenvectors of ψ_k vary significantly across groups and $\lambda_1 \gg \lambda_2$, the subspace accuracy can far exceed this benchmark (blue). Intuitively, when the first eigenvectors of two different groups are nearly orthogonal, each group provides a lot of information about orthogonal directions on VV^T and so the gains in accuracy exceed those that you would get by estimating the subspace from a single group with K times the sample size. In general the accuracy of shared subspace estimates depends on the variation in the eigenvectors of ψ_k across groups as well as the magnitude of the eigenvalues and matrix dimensions p and n_k . Although the shared subspace estimator improves on the accuracy of individually estimated covariance matrices, estimates can still be biased when γ is very large or the eigenvalues of Σ_k are very small for all k . In practice, one should estimate the approximate magnitude of the bias using the inferred eigenvalues of Σ_k . When these inferred eigenvalues are significantly larger than $\hat{\sigma}_k^2(1 + \sqrt{\gamma/K})$ the bias will likely be small.

6 Analysis of Biological Data

In this Section we apply shared subspace spiked covariance models to data in two different biological examples. In the first, we compare gene expression data from juveniles with different subtypes of leukemia. Even after removing mean effects, our results indicate significant differences in covariance matrices between groups. In the second example, we compare covariance matrices in a metabolomic analysis of *Drosophila* data. In this example, after controlling for mean effects due to fly age, sex and genotype, we find little compelling evidence of differences in metabolite covariances between groups.

In these analyses we employ a shared subspace model in which we define the s by s matrix Ψ_k as

$$\Psi_k = \begin{pmatrix} O_k \Lambda_k O_k^T & 0 \\ 0 & D \end{pmatrix} \quad (17)$$

For the following analyses $O_k \Lambda_k O_k^T$ is a rank $r = 2$ matrix and D is an $(s - r)$ -dimensional diagonal matrix. We write $V = [V_1, V_2]$, with $V_1 \in \mathcal{V}_{p,r}$ as the basis for an r -dimensional shared subspace that explains the differences between groups and $V_2 \in \mathcal{V}_{p,(s-r)}$ corresponding to the remaining $(s - r)$ eigenvectors common to all groups. Importantly, we make no assumptions about the magnitude

of the eigenvalues Λ_k relative to the eigenvalues D , so that the largest eigenvectors of Ψ_k may correspond to the eigenvalues from columns of V_2 .

We find this formulation useful because in real world analyses, differences between groups may not manifest themselves in the first principal components. For instance, in genetic analyses, there may be large between subject variability common to all groups which is unrelated to how those subjects are grouped. Differences between groups may manifest themselves in the smaller principal components. This formulation allows a complete pooling of several eigenvectors, in addition to a space to identify and compare relevant differences. Using this framework we can easily visualize and compare the largest differences between groups in a two dimensional space while completely pooling remaining anisotropic variability that is not specific to the grouping.

Analysis of Gene Expression Data: We demonstrate the utility of the shared subspace covariance estimator for exploring differences in the covariability of gene expression levels in young adults with different subtypes of pediatric acute lymphoblastic leukemia [Yeoh et al., 2002]. The raw data consists of gene expression levels for thousands of genes in seven different subtypes of leukemia: BCR-ABL, E2A-PBX1, Hyperdip50, MLL, T-ALL, TEL-AML1 and a seventh group for unidentified subtypes (“Others”). The groups have corresponding sample sizes of $n = (15, 27, 64, 20, 43, 79, 79)$. Although there are over 12,000 genes in the dataset, the vast majority of expression levels are missing. Thus, we restrict our attention to the genes for which less than half of the values are missing and use Amelia, a software package for missing value imputation, to fill in the remaining missing values [Honaker et al., 2011]. After restricting the data in this way, $p = 3124$ genes remain. Prior to analysis, we demean both the rows and columns of the gene expression levels in each group.

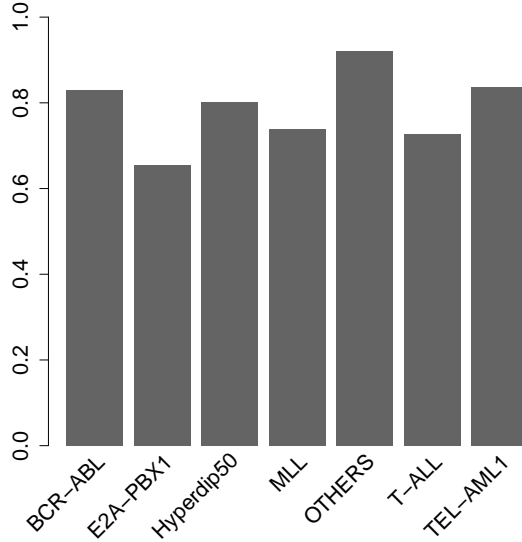
In Figure 5 we plot the results of our analysis. Panel 5(a) shows that over 60% of the estimated variation in the top s eigenvectors of Σ_k can be explained by the shared subspace for all groups, with over 80% explained in 4 of the 6 groups. Panel 5(b) reflects some significant differences in the posterior distribution of eigenvalues and eigenvectors between groups. The x -axis corresponds to the orientation of the principal axis of Ψ_k on \hat{V}_1 and the y -axis corresponds to the log ratio of the first two eigenvalues. Several groups have significantly different orientations for the first principal component of the projected covariance matrix, as well as differences in the ratio of eigenvalues. For instance, the subtype E2A-PBX1 has a larger eigenvalue ratio which reflects a more correlated distribution on this subspace. The posterior regions for the TEL-AML1 and Hyperdip50 groups are almost entirely overlapping, which suggests there is little detectable difference between their

covariance structures. Note that when the eigenvalue ratio is close to one (as is the case for the “other” subtype), the distribution of expression values on the subspace is nearly spherical and thus the orientation of the primary eigenvector is at best weakly identifiable. This is reflected in the wide posterior range of orientations of the first principal component.

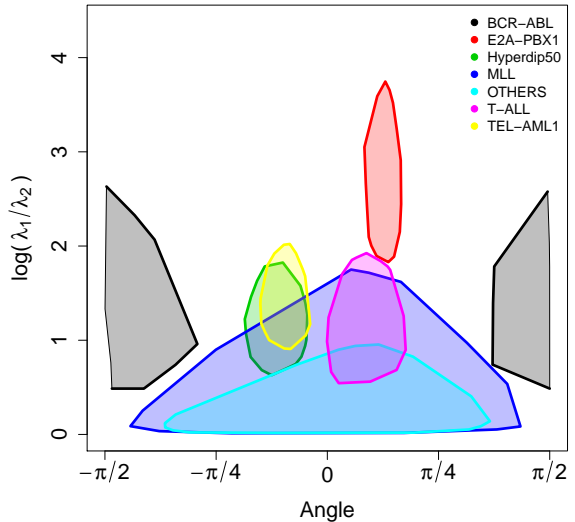
Further intuition about the differences in covariances between groups can be understood in the biplot in Figure 6. Here, we plot the contours of the covariance matrices for three leukemia subtypes. The 1% of genes with the largest loadings on the first two columns of \hat{V}_1 are indicated with black shapes and the remaining loadings with light grey dots. The genes with the largest loadings are clustered by quadrant and listed in the corresponding table. Even though we remove all mean-level differences in gene expressions between groups, we are still able to identify genes with known connections to cancer and leukemia. As one example, MYC (top right) is an oncogene with well established association to many cancers [Dang, 2012].

In this figure, genes that fall in the upper right quadrant have positive loadings in both columns of \hat{V}_1 . Genes in the upper left corner of the figure have positive loadings on the first column of \hat{V}_1 but negative loadings on the second column of \hat{V}_1 . The principal axis for a group aligns in the direction of genes that exhibit the largest variability in that group. Genes which lie in a direction orthogonal to the principal axis exhibit reduced variability, relative to the other groups. As an example, genes in the upper left corner of this plot (triangles) exhibit large, positively correlated variability in the Hyperdip50 group. In this same group, there is reduced variability, relative to the other groups, among the genes in the upper right corner of the plot (squares), since this cluster of genes lie in a direction nearly orthogonal to the principal axis. In contrast, the BCR-ABL group is aligned primarily with the second column of \hat{V}_1 , which means that the genes indicated by squares and circles vary significantly in this group. Genes in the square group are anti-correlated with those in the circle group, since their loadings have opposite signs on the second column of \hat{V}_1 .

Analysis of Metabolomic Data: Next, we briefly discuss an example in which we could not readily identify significant covariance differences between groups. Here, we apply shared subspace group covariance estimation to a metabolomic data analysis on fly aging [Hoffman et al., 2014]. We bin the data to include groups of flies less than 10 days (young), between 10 and 51 days (middle) and greater than 51 days (old), and further split by sex. The sample sizes range from 43 to 59 flies per group. We analyze metabolomic data corresponding to metabolites with 3714 mass-charge ratios. After removing mean effects due to age and sex, we fit the shared subspace estimator



(a) $\gamma(Y_k : \hat{V}, \hat{\sigma}_k^2)$



(b) 95% Posterior Regions

Figure 5: a) Goodness of shared subspace fit for each of the seven Leukemia groups. The subspace explains over 60% of the estimated variation in the top s eigenvectors of Σ_k in each of the seven groups, with more than 80% explained in most groups. b) 95% posterior regions for the eigenvalue ratio and primary eigenvector orientation. Regions for some pairs of groups are disjoint, suggesting significant differences in the projected covariance matrices. For other groups (e.g. Hyperdip50 and TEL-AML1) overlap in the posterior regions indicate that differences are not detectable on this subspace.

and compare covariances between groups. We identify a subspace that explains almost all of the variability in the first few components of Σ_k for all groups (Figure 7(a)) but see little evidence for differences in metabolite covariances on this subspace, as evidenced by the large overlap in posterior distributions for each group (Figure 7(b)). This could be indicative of a large amount of variation that is common across all groups for the first s principal components. Differences in covariation across groups, if there are any, likely manifest themselves in the smaller principal components that are too small to detect given the sample sizes.

7 Discussion

In this paper, we proposed a class of models for estimating and comparing differences in covariance matrices across multiple groups on a common low dimensional subspace. We described an empirical

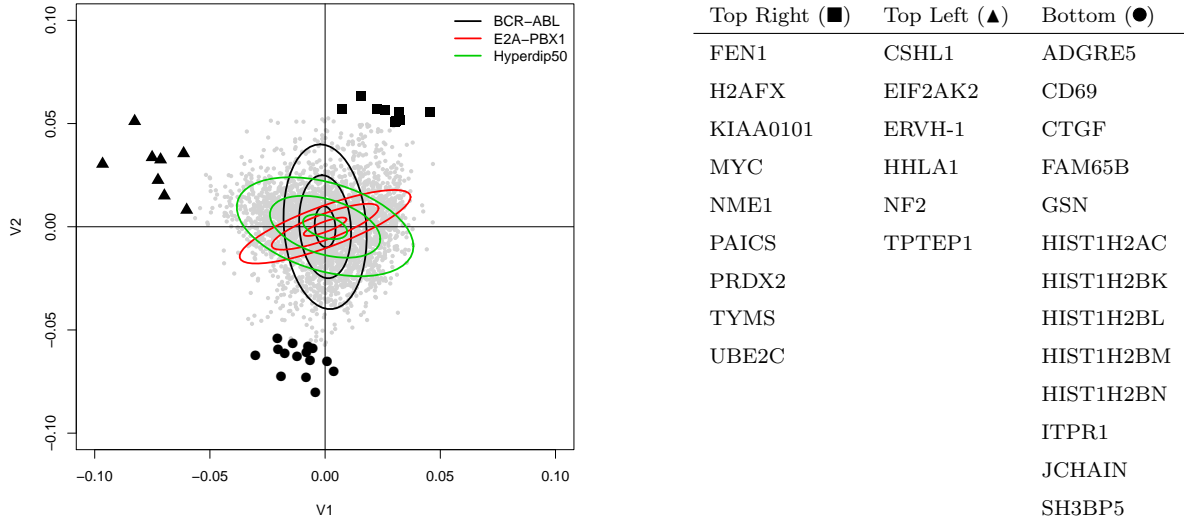
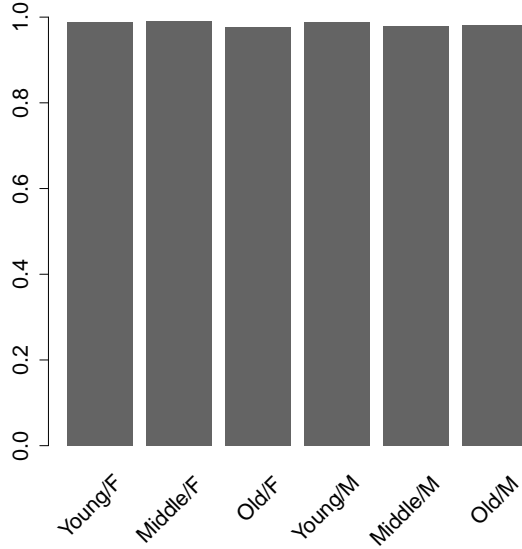


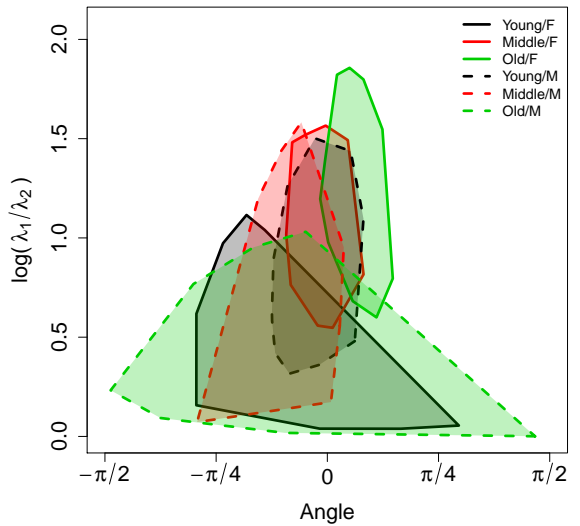
Figure 6: Left) Variant of a biplot with contours for three leukemia subtypes and the loadings for each gene on the first two columns of \hat{V} . The loadings for all of the genes are displayed in light gray, and the top 1% of genes with with the largest magnitude loadings are displayed as either a triangle, square or circle depending on which quadrant they lie in. Right) List of the gene's with the largest loadings, grouped by quadrant.

Bayes algorithm for estimating this common subspace and a Gibbs sampler for inferring the projected covariance matrices and their associated uncertainty. Estimates of both the shared subspace and the projected covariance matrices can both be useful summaries of the data. For example, with the biological data, the shared subspace highlights the full set of genes or metabolites that are correlated across groups. Differences between group covariance matrices can be understood in terms of differences in these sets of correlated molecules. In analyses of these datasets, we demonstrated how we can use these notions to visualize and contrast the posterior distributions of covariance matrices projected onto a particular subspace.

In simulation, we showed that the shared subspace model can still be a reasonable choice for modeling multi-group covariance matrices even when the groups may be largely dissimilar. When there is little similarity between groups, the shared subspace model can still be appropriate as long as the dimension of the shared subspace is large enough. However, selecting the rank of the shared subspace remains a practical challenge. Although we propose a useful heuristic for choosing the dimension of the shared subspace based on the rank selection estimators of Gavish and Donoho [2014], a more principled approach is warranted. Improved rank estimators would further improve



(a) $\gamma(Y_k : \hat{V}, \hat{\sigma}_k^2)$



(b) 95% Posterior Regions

Figure 7: a) Goodness of fit is close to one for all groups suggesting that the inferred subspace preserves most of the variability across groups. b) There is significant overlap in the posterior distribution of the log eigenvalue ratio and primary eigenvector orientation across groups. Thus, there is little evidence of significant differences in the covariance matrices between groups on this inferred subspace.

the performance of the adaptive shared subspace estimator discussed in Section 4.

It is also a challenging problem to estimate the “best” subspace once the rank of the space is specified. We used maximum marginal likelihood to estimate VV^T and then used MCMC to infer Ψ_k . By focusing on group differences for Ψ_k on a *fixed* subspace, it is much simpler to interpret similarities and differences. Nevertheless, full uncertainty quantification for VV^T can be desirable. We found MCMC inference for VV^T to be challenging for the problems considered in this paper and leave it for future work to develop an efficient fully Bayesian approach for estimating the joint posterior of VV^T and Ψ_k . Recently developed Markov chain Monte Carlo algorithms, like Riemmanian manifold Hamilton Monte Carlo, which can exploit the geometry of the Grassmann manifold, may be useful here [Byrne and Girolami, 2013, Girolami and Calderhead, 2011]. It may also be possible, though computationally intensive, to jointly estimate s and VV^T using for instance, a reversible-jump MCMC algorithm.

Fundamentally, our approach is quite general and can be integrated with existing approaches for multi-group covariance estimation. In particular, we can incorporate additional shrinkage on the

projected covariance matrices Ψ_k . As in Hoff [2009a] we can employ non-uniform Bingham prior distributions for the eigenvectors of Ψ_k or we can model Ψ_k as a function of continuous covariates as in Yin et al. [2010] and Hoff and Niu [2012]. Alternatively, we can summarize the estimated covariance matrices by thresholding entries of the precision matrix, Ψ_k^{-1} to visualize differences between groups using a graphical model [Meinshausen and Bühlmann, 2006]. The specifics of the problem at hand should dictate which shrinkage models are appropriate, but the shared subspace assumption can be useful in a wide range of analyses, especially when the number of features is very large. A repository for the replication code is available on GitHub [Franks, 2016].

References

Jinho Baik and Jack W. Silverstein. Eigenvalues of large sample covariance matrices of spiked population models. *Journal of Multivariate Analysis*, 97(6):1382–1408, 2006. ISSN 0047259X. doi: 10.1016/j.jmva.2005.08.003. URL <http://linkinghub.elsevier.com/retrieve/pii/S0047259X0500134X>.

Matthew Barker and William Rayens. Partial least squares for discrimination. *Journal of Chemometrics*, 17(3):166–173, 2003. ISSN 08869383. doi: 10.1002/cem.785. URL <http://dx.doi.org/10.1002/cem.785>.

Robert J Boik. Spectral models for covariance matrices. *Biometrika*, 89(1):159–182, 2002.

Simon Byrne and Mark Girolami. Geodesic Monte Carlo on embedded manifolds. *Scandinavian Journal of Statistics*, 40(4):825–845, 2013.

Yasuko Chikuse. *Statistics on special manifolds*, volume 174. Springer Science & Business Media, 2012.

Patrick Danaher, Pei Wang, and Daniela M. Witten. The joint graphical lasso for inverse covariance estimation across multiple classes. *Journal of the Royal Statistical Society. Series B: Statistical Methodology*, 76(2):373–397, 2014. ISSN 13697412. doi: 10.1111/rssb.12033.

Chi V Dang. Myc on the path to cancer. *Cell*, 149(1):22–35, 2012.

David L Donoho, Matan Gavish, and Iain M Johnstone. Optimal shrinkage of eigenvalues in the spiked covariance model. *arXiv preprint arXiv:1311.0851*, 2013.

Morris L Eaton. Group invariance applications in statistics. In *Regional conference series in Probability and Statistics*, pages i–133. JSTOR, 1989.

BK Flury. Two generalizations of the common principal component model. *Biometrika*, 74(1):59–69, 1987. ISSN 00063444. doi: 10.2307/2336021. URL <http://biomet.oxfordjournals.org/content/74/1/59.short>.

Alexander M. Franks. Shared Subspace Estimation. <https://github.com/afranks86/shared-subspace>, 2016.

Matan Gavish and David L Donoho. The optimal hard threshold for singular values is $4/\sqrt{3}$. *Information Theory, IEEE Transactions on*, 60(8):5040–5053, 2014.

Mark Girolami and Ben Calderhead. Riemann manifold Langevin and Hamiltonian Monte Carlo methods. *Journal of the Royal Statistical Society. Series B: Statistical Methodology*, 73:123–214, 2011. ISSN 13697412. doi: 10.1111/j.1467-9868.2010.00765.x.

Graham Heimberg, Rajat Bhatnagar, Hana El-Samad, and Matt Thomson. Low dimensionality in gene expression data enables the accurate extraction of transcriptional programs from shallow sequencing. *Cell Systems*, 2(4):239–250, 2016.

Peter D Hoff. A hierarchical eigenmodel for pooled covariance estimation. *Journal of the Royal Statistical Society: Series B (Statistical Methodology)*, 71(5):971–992, 2009a.

Peter D Hoff. Simulation of the matrix Bingham–von Mises–Fisher distribution, with applications to multivariate and relational data. *Journal of Computational and Graphical Statistics*, 2009b.

Peter D Hoff and Xiaoyue Niu. A covariance regression model. *Statistica Sinica*, 22:729–753, 2012.

Jessica M Hoffman, Quinlyn A Soltow, Shuzhao Li, Alfire Sidik, Dean P Jones, and Daniel EL Promislow. Effects of age, sex, and genotype on high-sensitivity metabolomic profiles in the fruit fly, *drosophila melanogaster*. *Aging cell*, 13(4):596–604, 2014.

James Honaker, Gary King, and Matthew Blackwell. Amelia II: A program for missing data. *Journal of Statistical Software*, 45(7):1–47, 2011. URL <http://www.jstatsoft.org/v45/i07/>.

Iain M Johnstone. On the distribution of the largest eigenvalue in principal components analysis. *Annals of statistics*, pages 295–327, 2001.

CG Khatri and KV Mardia. The von Mises-Fisher matrix distribution in orientation statistics. *Journal of the Royal Statistical Society. Series B (Methodological)*, pages 95–106, 1977.

J Kiefer and R Schwartz. Admissible Bayes character of T_2 -, R_2 -, and other fully invariant tests for classical multivariate normal problems. *The Annals of Mathematical Statistics*, pages 747–770, 1965.

Kantilal Varichand Mardia, John T Kent, and John M Bibby. *Multivariate analysis*. Academic press, 1980.

Nicolai Meinshausen and Peter Bühlmann. High-dimensional graphs and variable selection with the lasso. *The annals of statistics*, pages 1436–1462, 2006.

Debashis Paul. Asymptotics of sample eigenstructure for a large dimensional spiked covariance model. *Statistica Sinica*, pages 1617–1642, 2007.

James R Schott. Some tests for common principal component subspaces in several groups. *Biometrika*, 78(4):771–777, 1991.

James R Schott. Partial common principal component subspaces. *Biometrika*, 86(4):899–908, 1999.

Michael E Tipping and Christopher M Bishop. Probabilistic principal component analysis. *Journal of the Royal Statistical Society: Series B (Statistical Methodology)*, 61(3):611–622, 1999.

Zaiwen Wen and Wotao Yin. A feasible method for optimization with orthogonality constraints. *Mathematical Programming*, 142(1-2):397–434, 2013.

Svante Wold, Michael Sjöström, and Lennart Eriksson. Pls-regression: a basic tool of chemometrics. *Chemometrics and intelligent laboratory systems*, 58(2):109–130, 2001.

Eng-Juh Yeoh, Mary E Ross, Sheila A Shurtleff, W Kent Williams, Divyen Patel, Rami Mahfouz, Fred G Behm, Susana C Raimondi, Mary V Relling, Anami Patel, et al. Classification, subtype discovery, and prediction of outcome in pediatric acute lymphoblastic leukemia by gene expression profiling. *Cancer cell*, 1(2):133–143, 2002.

Jianxin Yin, Zhi Geng, Runze Li, and Hansheng Wang. Nonparametric covariance model. *Statistica Sinica*, 20:469, 2010.